Supplementary Material for The Potential of Zero Total Charge and Electrocatalytic Properties of Ru@Pt Core-Shell Nanoparticles

Jørgen Svendby Frode Seland Gurvinder Singh
José Luis Gómez de la Fuente
Svein Sunde*

Department of Materials Science and Engineering, Norwegian University of Science and Technology (NTNU), NO-7491 Trondheim, Norway

October 24, 2018

*Corresponding author. Tel.: +47 73594051; fax: +47 73591105, *E-mail address:* svein.sunde@ntnu.no

S1 Determination of potential of zero charge for Ru@Pt/C in $HClO_4$ and H_2SO_4

Fig. S.1 shows the result of the CO-charge displacement technique measurement of Ru@Pt/C in 0.1 mol dm^{-3} $HClO_4$. As can be seen, the current peaks go from being predominantly positive to being predominantly negative with increasing potential. Net charges for the different potentials were obtained by integration of the currents from the point of admission of CO to the cell until the point at which the current had again reached a stable value. The current prior to the admission of CO systematically decreased with decreasing potential. However, in 0.5 mol dm^{-3} H_2SO_4 we found the misalignment to be negligible at any potential in 0.5 mol dm^{-3} H_2SO_4 during similar experiments, Fig. S.2. The small cathodic currents at Ru@Pt at low potential in the perchloric acid solutions are possibly due to reduction of perchlorate [3, 7, 9]. To eliminate the effect of these, the integration was performed after subtraction of a (linear) sloped baseline from the current just prior to admission of the CO to the stable value of the current obtained after all transients due to the CO admission had decayed in perchlorate solutions. We observed no misalignment in our measurements for Pt/C in perchloric acid at any potential, indicating that any perchlorate reduction at Ru@Pt would be catalytic in nature.

Fig. S.3 presents the integrated charges plotted versus the applied potential in 0.1 mol dm^{-3} $HClO_4$ with a fitted straight line; we use the convention that y is plotted *versus* x. We estimate the PZTC-value for Ru@Pt/C to be 0.14 V vs. RHE from the intercept of the line with the potential axis. This value lies between the reported PZTC-values for Pt/C and PtRu/C in 0.1 mol dm^{-3} $HClO_4$ solutions, which are 0.27 V[12] and 0.042 V[8] vs. RHE, respectively. Note also that the PZTC can be determined from one single value of the displacement charge alone, for example that at 0.18 V in $HClO_4$ for which the misalignment is minimal, and the cyclic voltammogram [11, 6]. This gives a similar value for the PZTC to that obtained by the interpolation procedure in Fig. S.3.

Fig. S.4 compares the charge integrated from the CV with the charges measured by displacement. The slope from the voltammogram is slightly larger than that of the displacement charge. Overall the agreement is good, however.

Displacement charges were also measured in sulfuric acid. A plot of dis-

placed charges in 0.5 mol dm^{-3} H_2SO_4 as a function of potential is shown in Fig. S.5. This plot indicates a slightly higher value for the PZTC than in perchloric acid (approximately 0.16 V), but still substantially lower than those for Pt in sulfuric acid (by approximately 150 mV [14]).

Fig. S.6 shows a voltammogram for Ru@Pt in 0.5 mol dm^{-3} H_2SO_4. The voltammetric charge from the voltammograms are compared to the charge from the displacement measurements in Fig. S.7. The displacement charges and those from the voltammograms are again quite close for both sweep rates.

Fig. S.7 shows the charge obtained by integration of the voltammogram for Ru@Pt in 0.5 mol dm^{-3} H_2SO_4.

S2 Cyclic voltammograms in $HClO_4$ normalised with respect to CO-stripping charge

Cyclic voltammograms for Ru@Pt/C and Pt/C normalised with respect to the CO-stripping charge are shown in Fig. S.8.

S3 PZTC vs. PZFC in the presence of two adsorption processes

The displacement charge is

$$Q_{\mathrm{d}}(E) = -\sigma(E) + F\Gamma_{\mathrm{H}}(E) - F\Gamma_{\mathrm{OH}}(E) \tag{S.1}$$

We consider the reactions determining the last two terms in Eq. (S.1) to be

$$\mathrm{H_2O}(\ell) + \square_{\mathrm{ad}} \rightleftharpoons \mathrm{OH_{ad}} + \mathrm{H^+(aq)} + \mathrm{e^-(Pt)} \tag{S.2}$$

$$\mathrm{H^+(aq)} + \mathrm{e^-(Pt)} + \square_{\mathrm{ad}} \rightleftharpoons \mathrm{H_{ad}} \tag{S.3}$$

in perchloric acid, where $\square_{\mathrm{ad}}$ is a vacant catalyst surface site. We assume that the potential is measured with respect to a reversible hydrogen electrode (RHE), at which

$$\mathrm{H^+(aq)} + \mathrm{e^-(Pt')} \rightleftharpoons \frac{1}{2}\mathrm{H_2(g)} \tag{S.4}$$

Thus we may write cell reactions corresponding to Eqs. (S.2) through (S.4)

$$\mathrm{H_2O}(\ell) + \square_{\mathrm{ad}} + \mathrm{e^-(Pt')} \;\rightleftharpoons\; \mathrm{OH_{ad}} + \frac{1}{2}\mathrm{H_2(g)} + \mathrm{e^-(Pt)} \tag{S.5}$$

$$\frac{1}{2}\mathrm{H_2(g)} + \square_{\mathrm{ad}} + \mathrm{e^-(Pt)} \;\rightleftharpoons\; \mathrm{e^-(Pt')} + \mathrm{H_{ad}} \tag{S.6}$$

For Eq. (S.5)

$$\tilde{\mu}'_{\mathrm{e}} - \tilde{\mu}_{\mathrm{e}} = \tilde{\mu}_{\mathrm{OH}} + \frac{1}{2}\tilde{\mu}_{\mathrm{H_2}} - \tilde{\mu}_{\mathrm{H_2O}} - \tilde{\mu}_{\square} \tag{S.7}$$

or upon expansion of the electrochemical potentials

$$\begin{aligned} FE = F\left(\phi_{\mathrm{Pt}} - \phi_{\mathrm{Pt'}}\right) = \tilde{\mu}_{\mathrm{OH}} - \tilde{\mu}_{\mathrm{H_2O}} - \tilde{\mu}_{\square} = \\ = \Delta G^0_{\mathrm{OH}} + RT \ln\left\{\frac{a_{\mathrm{OH}}}{a_{\square}}\right\} \\ = \Delta G^0_{\mathrm{OH}} + RT \ln\left\{\frac{\theta_{\mathrm{OH}}}{1-\theta_{\mathrm{H}}-\theta_{\mathrm{OH}}}\right\} \end{aligned} \tag{S.8}$$

if $\tilde{\mu}^0_{\mathrm{H_2}} = 0$ (and unit activity of $\mathrm{H^+}$), $a_{\mathrm{H_2O}} = 1$, and with

$$\Delta G^0_{\mathrm{OH}} = \mu^0_{\mathrm{OH}} - \mu^0_{\mathrm{H_2O}} - \mu^0_{\square} \tag{S.9}$$

For Eq. (S.6) we obtain in a similar fashion

$$\tilde{\mu}'_{\mathrm{e}} - \tilde{\mu}_{\mathrm{e}} = \frac{1}{2}\tilde{\mu}_{\mathrm{H_2}} + \tilde{\mu}_{\square} - \tilde{\mu}_{\mathrm{H}} \tag{S.10}$$

$$\begin{aligned} FE = F\left(\phi_{\mathrm{Pt}} - \phi_{\mathrm{Pt'}}\right) = \tilde{\mu}_{\square} - \tilde{\mu}_{\mathrm{H}} = -\Delta G^0_{\mathrm{H}} + RT \ln\left\{\frac{a_{\square}}{a_{\mathrm{H}}}\right\} \\ = -\Delta G^0_{\mathrm{H}} + RT \ln\left\{\frac{1-\theta_{\mathrm{H}}-\theta_{\mathrm{OH}}}{\theta_{\mathrm{H}}}\right\} \end{aligned} \tag{S.11}$$

again if $\tilde{\mu}^0_{\mathrm{H_2}} = 0$ (and unit activity of $\mathrm{H^+}$), $a_{\mathrm{H_2O}} = 1$, and with

$$\Delta G^0_{\mathrm{H}} = \mu^0_{\mathrm{H}} - \mu^0_{\square} \tag{S.12}$$

Adding Eqs. (S.8) and (S.11) gives

$$\frac{\theta_{\mathrm{OH}}}{\theta_{\mathrm{H}}} = \exp\left\{\frac{2FE - [-\Delta G^0_{\mathrm{H}} + \Delta G^0_{\mathrm{OH}}]}{RT}\right\} \tag{S.13}$$

Combining Eqs. (S.8), (S.11) and (S.13) gives upon rearrangement,

$$\theta_{\mathrm{OH}} = \frac{1}{\exp\left\{-\frac{FE-\Delta G^0_{\mathrm{OH}}}{RT}\right\} + \exp\left\{-\frac{2FE-\left[-\Delta G^0_{\mathrm{H}}+\Delta G^0_{\mathrm{OH}}\right]}{RT}\right\} + 1} \tag{S.14}$$

and

$$\theta_{\mathrm{H}} = \frac{1}{\exp\left\{\frac{FE+\Delta G^0_{\mathrm{H}}}{RT}\right\} + \exp\left\{\frac{2FE-\left[-\Delta G^0_{\mathrm{H}}+\Delta G^0_{\mathrm{OH}}\right]}{RT}\right\} + 1} \tag{S.15}$$

Literature results indicate that ΔG^0_{H} and ΔG^0_{OH} vary with the degree of coverage [15, 10, 2, 5], but for the purposes here we may neglect these. The displacement charge may be calculated from Eqs. (S.14) and (S.15)

$$\frac{q_{\mathrm{d}}}{F\Gamma_{\mathrm{H}}} = -\frac{C_{\mathrm{d}}\left(E - E_{\mathrm{PZFC}}\right)}{F\Gamma_{\mathrm{H}}} + \theta_{\mathrm{H}} - \frac{\Gamma_{\mathrm{OH}}}{F\Gamma_{\mathrm{H}}}\theta_{\mathrm{OH}} \tag{S.16}$$

where we have assumed a constant differential capacitance C_{d} of the electrode.

Fig. S.9 shows a simulated displacement charge along with the true double-layer charge for a set of parameters for which the two adsorption processes overlap. Clearly, extrapolation of the displacement charge from the linear portion above the PZTC will not give the correct PZFC.

Fig. S.10 shows a simulated displacement charge similar to that in Fig. S.9 but with a stronger binding of OH to the surface, i.e. with a lower value for ΔG_{OH}, $\Delta G_{\mathrm{OH}}/RT = 2$. All the other parameters were kept the same. Clearly, the displacement charge curve crosses the abscissa at a lower potential and thus displays a lower PZTC.

S4 Impedance analysis in the pseudo-capacitive potential range

The impedance was fitted to model circuits to show that impedance data comply qualitatively with the behaviour expected for adsorption processes, whereas they do not comply with simple double layer charging even in the qualitative sense. We therefore fitted the data by minimisation of the object function

$$\chi^2 = \sum_i \left\{\left[Re\mathcal{C}_i - Re\mathcal{C}_m\left(j\omega_i\right)\right]^2 + \left[Im\mathcal{C}_i - Im\mathcal{C}_m\left(j\omega_i\right)\right]^2\right\} \tag{S.17}$$

where $Re\mathcal{C}_i$ is the real part of the complex capacitance for angular frequency ω_i, $Re\mathcal{C}_m\left(j\omega_i\right)$ is the corresponding calculated result from the model circuit, $Im\mathcal{C}_i$ is the imaginary part of the complex capacitance for angular frequency ω_i, and $Im\mathcal{C}_m\left(j\omega_i\right)$ is the corresponding calculated result from the model circuit. All data were fitted after subtraction of the series resistance.

A fit of the complex capacitance data to a simple capacitance gives a single point on the real axis in the complex-capacitance plane. For the data in Fig. 3 in the main article this value is 3×10^{-4} F.

A fit of the series-resistance subtracted complex-capacitance data to the following circuit

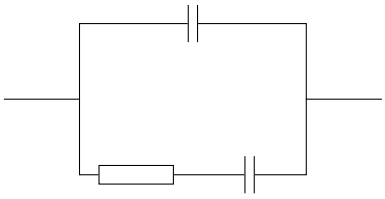

Equivalent circuit I

is presented in Fig. S.11.

As can be seen from the figure, the model gives a single arc in the complex-capacitance plot, whereas the data indicate at least two. We therefore also fitted the data to the following circuit,

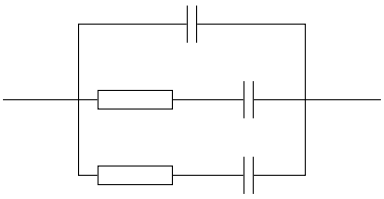

Equivalent circuit II

The result is presented in Fig. S.12 The fit improves, although refinements are obviously possible. This will not be pursued here, since the main objective has been to demonstrate that the circuits needed to represent the data are more complex than that corresponding to a simple double-layer, and do resemble those for faradaic adsorption processes at electrodes [4, 18]. Similar results were also obtained at 0.4 V.

S4.1 Adsorbate binding energy and electrocatalytic activity

To demonstrate the relation between binding energy of the adsorbate and electrocatalytic activity we use the reaction mechanism proposed by Nørskov and co-workers[13, 16]

$$\frac{1}{2}\mathrm{O_2} + \square_{\mathrm{ad}} \rightarrow \mathrm{O_{ad}} \tag{S.18}$$

$$\mathrm{O_{ad}} + \mathrm{H^+} + \mathrm{e^-} \rightarrow \mathrm{OH_{ad}} \tag{S.19}$$

$$\mathrm{HO_{ad}} + \mathrm{H^+} + \mathrm{e^-} \rightarrow \mathrm{H_2O} \tag{S.20}$$

where $\square_{\mathrm{ad}}$ is a vacant catalyst surface site. We assume an interdependence between the binding energies for OH and O, E_{OH} and E_{O}, respectively as expressed through the scaling relation $E_{\mathrm{OH}} = 0.50E_{\mathrm{O}} + 0.05$ [16]. Fig. S.13 shows the free energies of surface adsorbates for 1.23 V vs. RHE for the ORR for Pt and for a catalyst assuming a 40 kJ mol^{-1} (0.4 eV) decrease in the free energy of $\mathrm{OH_{ad}}$. The reaction step that determines the onset potential, the potential-determining step, for the ORR is the step with the largest uphill difference in ΔG [16, 13, 17]. For Pt, step (S.19) is thus obviously the potential-determining step, Fig. S.13. For a catalyst at which OH is more strongly bound to the surface the onset potential clearly increases with respect to that of platinum, in this case by some tenths of an electronvolt, corresponding approximately to the difference between Pt and Ru@Pt in the onset potential for the ORR in Fig. 4. The prediction from the assumption that the lower PZTC implies a more strongly bound OH is therefore that the Ru@Pt/C catalysts are inferior to the Pt/C for the ORR, in line with the experimental results.

References

[1] V. Climent and J. M. Feliu. Thirty years of platinum single crystal electrochemistry. *J. Solid State Electrochem.*, 15:1297–1315, 2011.

[2] Victor Climent, Roberto Gómez, José Orts, and Juan M. Feliu. Thermodynamic Analysis of the Temperature Dependence of OH Adsorption on Pt(111) and Pt(100) Electrodes in Acidic Media in the Absence of Specific Anion Adsorption. *J. Phys. Chem. B*, 110:11344–11351, 2006.

[3] F. Colom and M. J. González-Tejera. Reduction of Perchlorate Ion on Ruthenium Electrodes in Aqueous Solutions. *J. Electroanal. Chem.*, 190:243–255, 1985.

[4] B.E. Conway, J. Barber, and S. Morin. Comparative evaluation of surface structure specifcity of kinetics of UPD and OPD of H at single-crystal Pt electrodes. *Electrochimica Acta*, 44:1109–1125, 1998.

[5] N. R. Elzović, B. M. Babić, N. V. Kristajić, and Lj. M. Vračar. Specificity of the UPD of H to the structure of highly dispersed Pt on carbon support. *Int. J. Hydrogen Energy*, 32:1991 – 1998, 2007.

[6] Alberto Ganassin, Paula Sebastián, Víctor Climent, Wolfgang Schuhmann, Aliaksandr S. Bandarenka, and Juan Feliu. On the pH Dependence of the Potential of Maximum Entropy of Ir(111) Electrodes. *Scientific Reporst*, 7:1246–1–1246–14, 2017.

[7] G. Horányi and I. Bakos. Experimental evidence demonstrating the occurrence of reduction processes of ClO_4^- ions in an acid medium at platinized platinum electrodes. *J. Electroanal. Chem.*, 331:727–737, 1992.

[8] T.-Y. Jeon, K.-S. Lee, S. J. Yoo, Y.-H Cho, S. H. Kang, and Y.-E. Sung. Effect of surface segregation on the methanol oxidation reaction in carbon-supported Pt-Ru alloy nanoparticles. *Langmuir*, 26(11):9123–9129, 2010.

[9] G. G. Láng and G. Horányi. Some interesting aspects of the catalytic and electrocatalytic reduction of perchlorate ions. *J. Electroanal. Chem.*, 552:197–211, 2003.

[10] N. M. Marković, B. N. Grgur, and P. N. Ross. Temperature-Dependent Hydrogen Electrochemistry on Platinum Low-Index Single-Crystal Surfaces in Acid Solutions. *J. Phys. Chem. B*, 101:5405–5413, 1997.

[11] R. Martínez-Hincapié, P. Sebastián-Pascual, V. Climent, and J. M. Feliu. Investigating Interfacial Parameters with Platinum Single Crystal Electrodes. *Russ. J. Electrochem.*, 53:227–236, 2017.

[12] K. J. J. Mayrhofer, B. B. Blizanac, M. Arenz, V. R. Stamenkovic, P. N. Ross, and N. M. Marković. The Impact of Geometric and Surface Electronic Properties of Pt-Catalysts on the Particle Size Effect in Electrocatalysis. *J. Phys. Chem. B*, 109(30):14433–14440, 2005.

[13] J. K. Nørskov, J. Rossmeisl, Á. Logadóttir, L. Lindqvist, J. R. Kitchin, T. Bligaard, and H. Jónsson. Origin of the Overpotential for Oxygen Reduction at a Fuel-Cell Cathode. *J. Phys. Chem. B*, 108(46):17886–17892, 2004.

[14] O. A. Petrii. Zero Charge Potentials of Platinum Metals and Electron Work Functions (Review). *Russ. J. Electrochem.*, 49(5):401–422, 2013.

[15] P. N. Ross. Hydrogen chemisortion on Pt single crystal surfaces in acidic solutions. *Surf. Sci.*, 102:463–485, 1981.

[16] J. Rossmeisl, A. Logadóttir, and J. K. Nørskov. Electrolysis of water on (oxidized) metal surfaces. *Chem. Phys.*, 319:178–184, 2005.

[17] J. Rossmeisl, Z.-W. Qu, H. Zhu, G.-J. Kroes, and J. K. Nørskov. Electrolysis of water on oxide surfaces. *J. Electroanal. Chem.*, 607:83–89, 2007.

[18] K. J. P. Schouten, M. J. T. C. van der Niet, and M. T. M. Koper. Impedance spectroscopy of H and OH adsorption on stepped single-crystal platinum electrodes in alkaline and acidic media. *Physical Chemistry Chemical Physics*, 12:15217–15224, 2010.

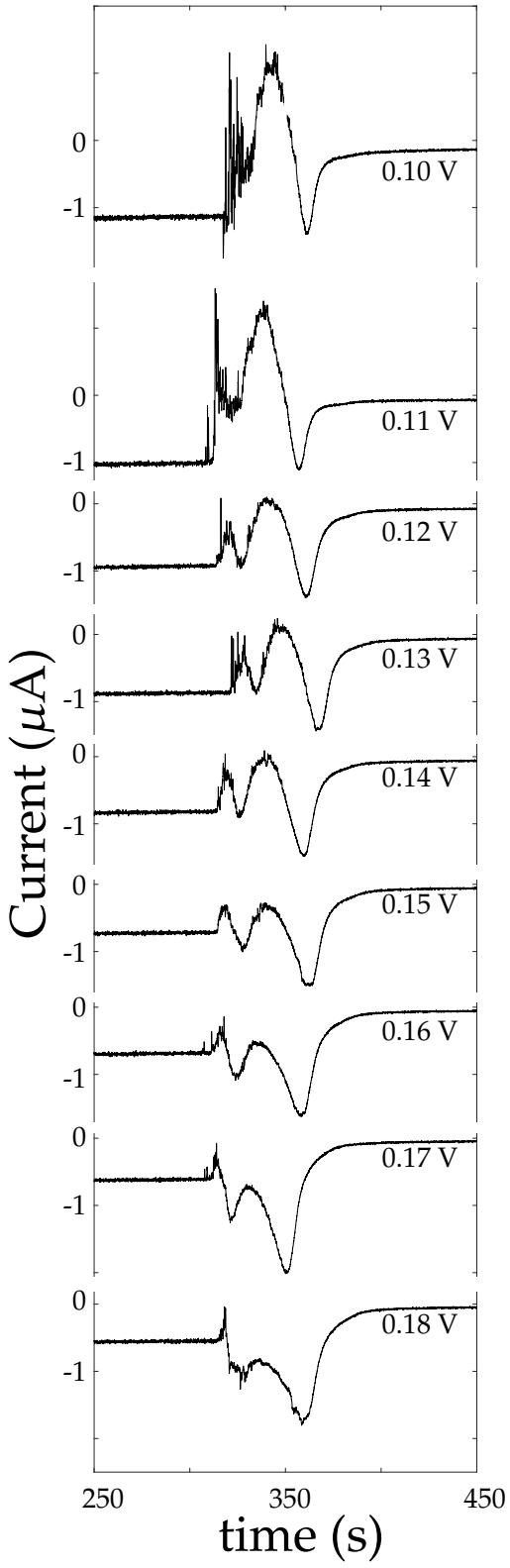

Figure S.1: CO-charge displacement currents for Ru@Pt/C at the given potential values in 0.1 mol dm^{-3} $HClO_4$ at 1000 rpm rotation.

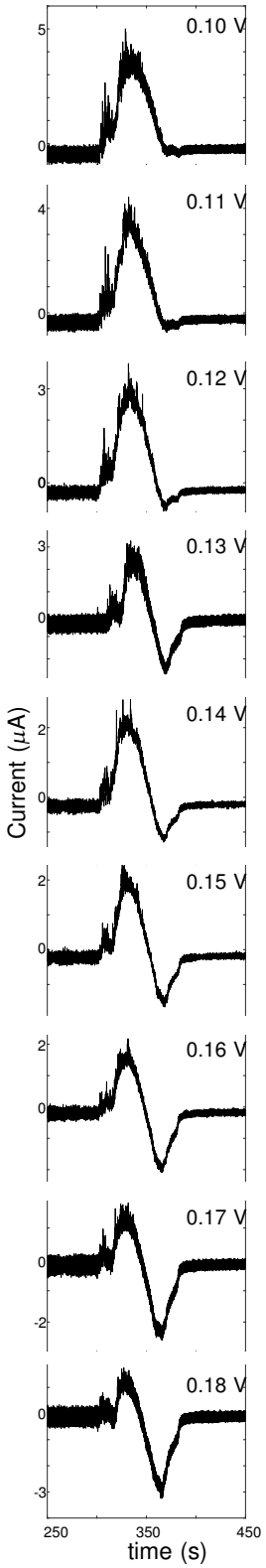

Figure S.2: CO-charge displacement currents for Ru@Pt/C at the given potential values in 0.5 mol dm^{-3} H_2SO_4 at 1000 rpm rotation.

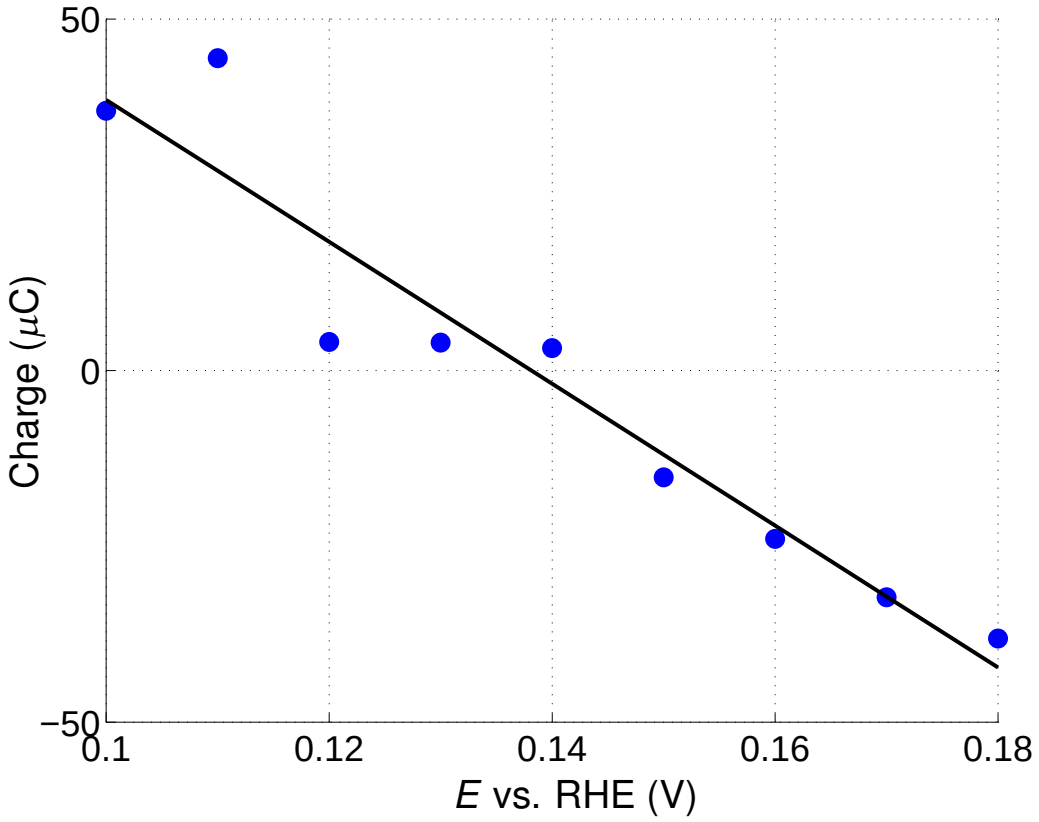

Figure S.3: Integrated charge values from the CO-charge displacement peaks vs. the applied potential in 0.1 mol dm^{-3} $HClO_4$.

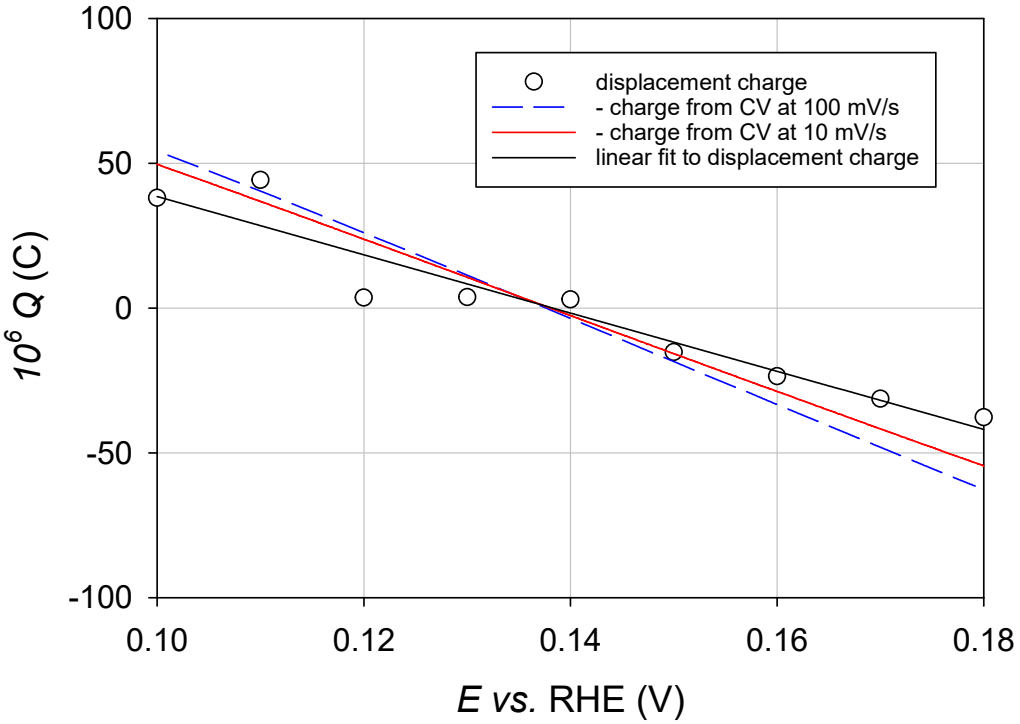

Figure S.4: Charge integrated through Eq. (2) in the main article from the voltammogram in Fig. 2b (line) and CO-charge displacement peaks (∘) vs. the applied potential in 0.1 mol dm^{-3} $HClO_4$. (The figure shows the negative of the charge from the voltammogram [1].)

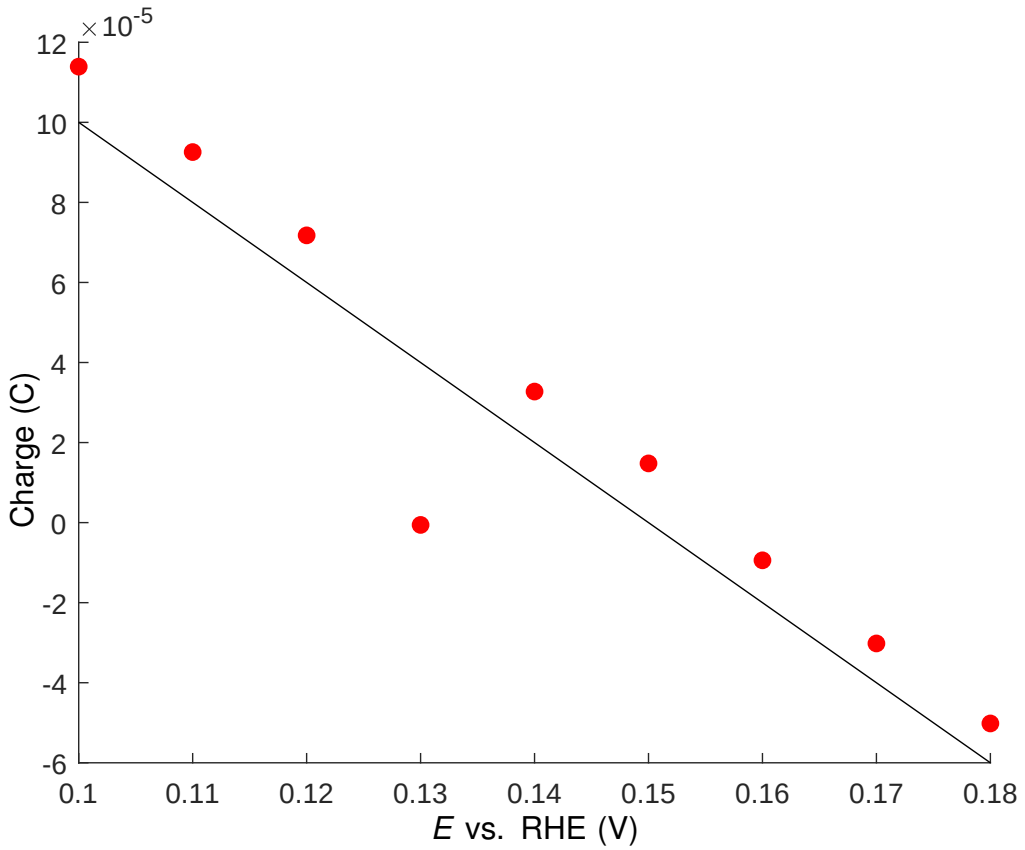

Figure S.5: Integrated charge values from the CO-charge displacement peaks vs. the applied potential in 0.5 mol dm^{-3} H_2SO_4.

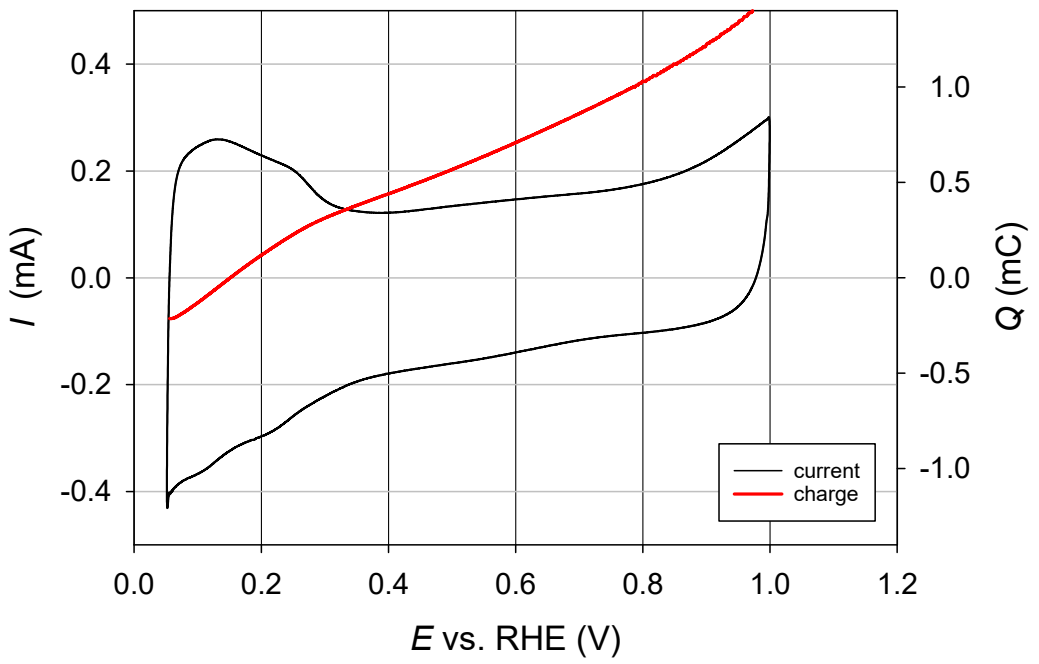

Figure S.6: Cyclic voltammogram for Ru@Pt recorded at 100 mV s^{-1} in 0.5 mol dm^{-3} H_2SO_4. The charge integrated through Eq. (2) in the main article is also shown in he figure.

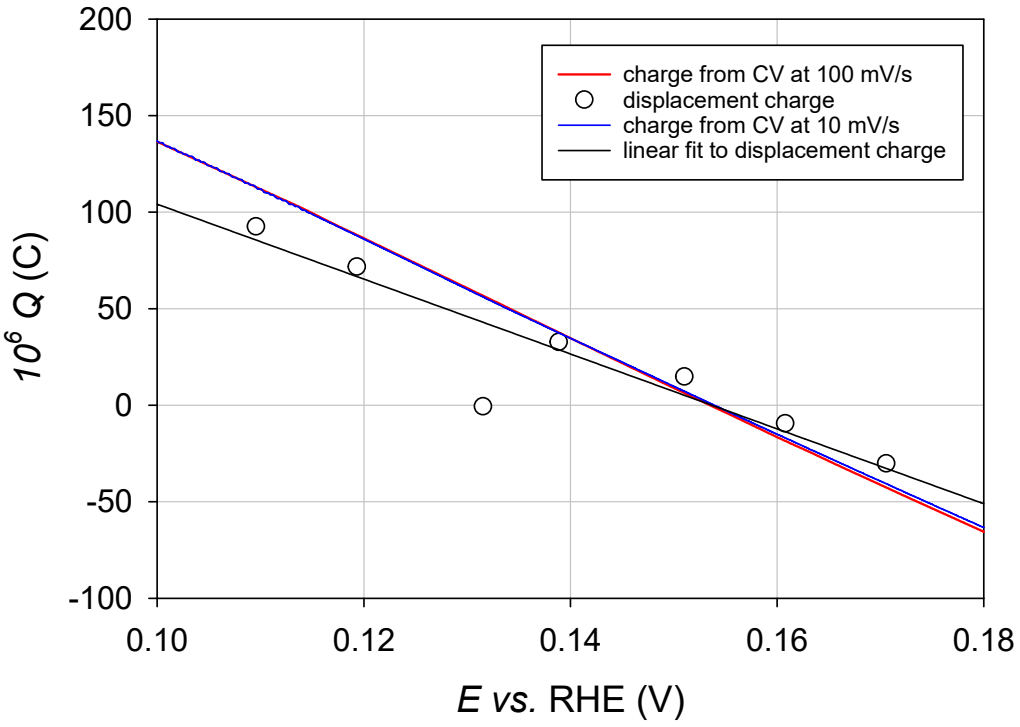

Figure S.7: Charge integrated through Eq. (2) in the main article from the voltammogram in Fig. S.6 recorded at 100 mV s^{-1} and a voltammogram recorded at 100 mV s^{-1} for Ru@Pt in 0.5 mol dm^{-3} H_2SO_4. (The charge from the voltammogram is shown with a negative sign.) Displacement charges from the CO-charge displacement measurements are included.

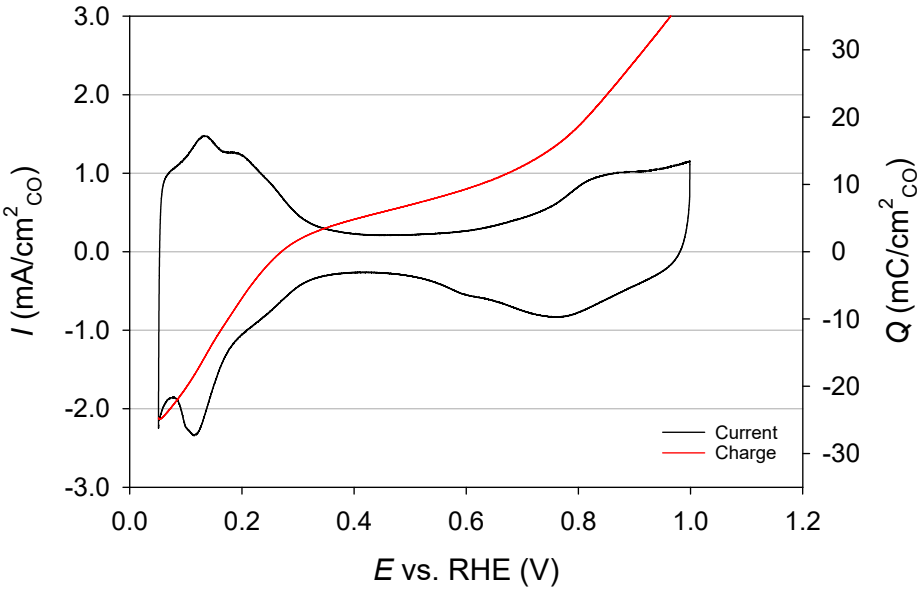

(a)

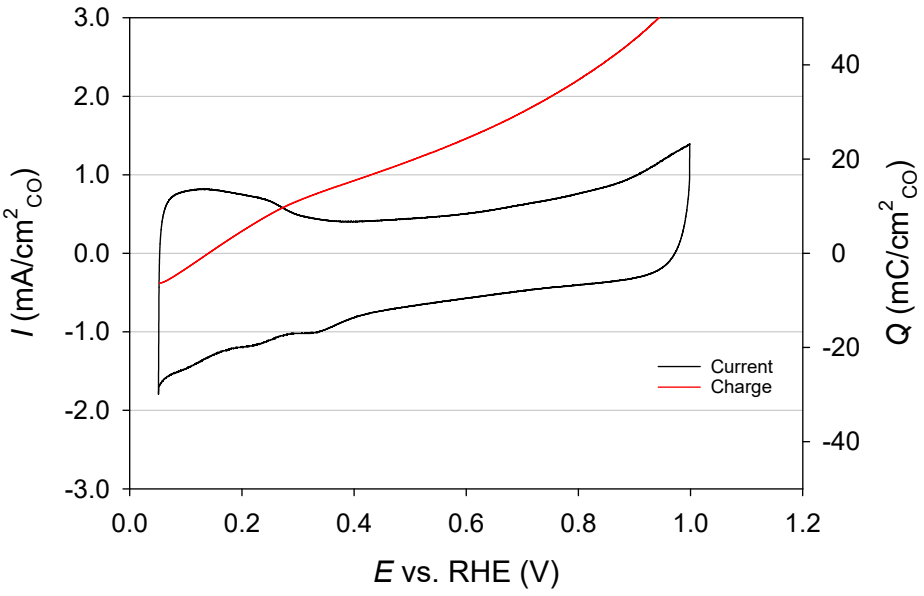

(b)

Figure S.8: 8(a) Cyclic voltammogram of Pt/C in 0.1 mol dm^{-3} $HClO_4$(aq) at a sweep rate of 10 mV s^{-1}, 8(b) Cyclic voltammogram of Ru@Pt/C in 0.1 mol dm^{-3} $HClO_4$(aq) at a sweep rate of 10 mV s^{-1}. The voltammetric charge Q_{CV} as calculated from Eq. (2) is shown for both voltammograms. The data were normalised with respect to CO-stripping charge.

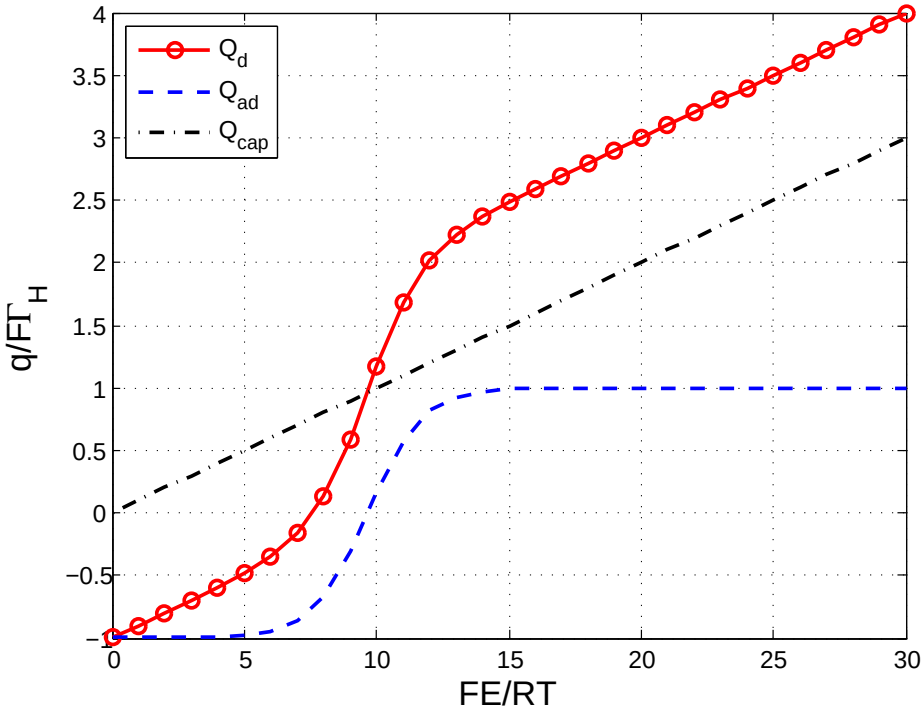

Figure S.9: Simulated dimensionless displacement charge for an electrode at which two adsorption processes takes place as a function of dimensionless potential. Parameters: $\Delta G_{\mathrm{OH}}/RT = 10$, $\Delta G_{\mathrm{H}}/RT = -10$, $C_{\mathrm{d}}\left(E - E_{\mathrm{PZFC}}\right)/F\Gamma_{\mathrm{H}} = 0.1$, $\Gamma_{\mathrm{OH}}/\Gamma_{\mathrm{H}} = 1$.

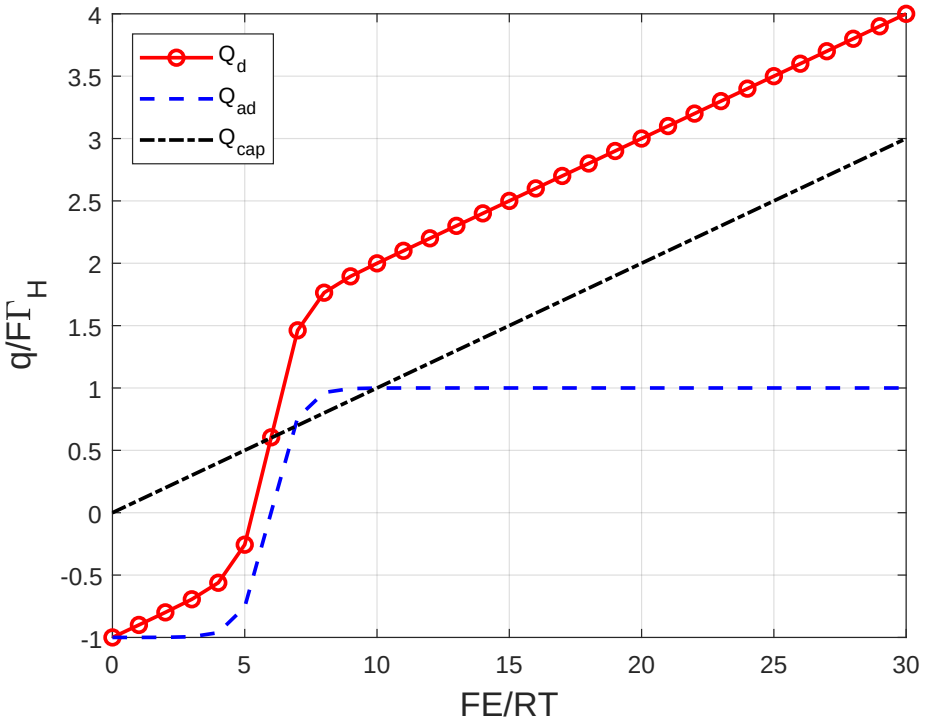

Figure S.10: Simulated dimensionless displacement charge for an electrode at which two adsorption processes takes place as a function of dimensionless potential. Parameters: $\Delta G_{\mathrm{OH}}/RT = 2$, $\Delta G_{\mathrm{H}}/RT = -10$, $C_{\mathrm{d}}\left(E - E_{\mathrm{PZFC}}\right)/F\Gamma_{\mathrm{H}} = 0.1$, $\Gamma_{\mathrm{OH}}/\Gamma_{\mathrm{H}} = 1$.

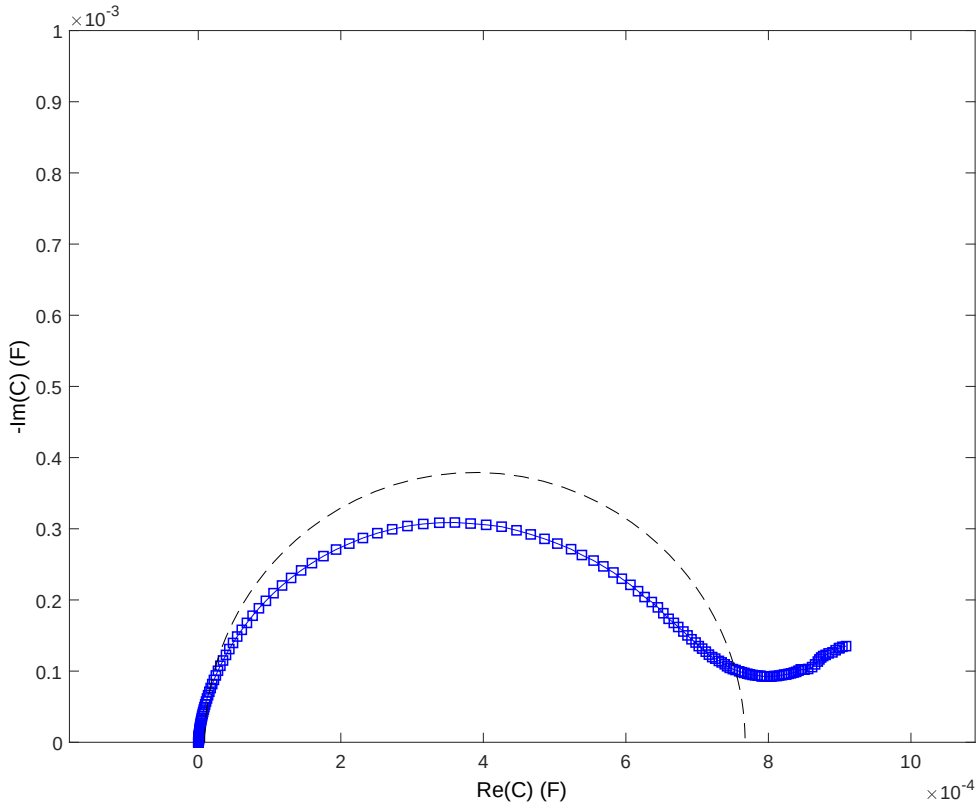

Figure S.11: Complex capacitance plot of a Ru@Pt/C catalyst at 0.5 V vs. RHE in 0.1 mol dm^{-3} $HClO_4$. The ohmic resistance was evaluated from the corresponding impedance-plane plot and subtracted from the data before calculating the complex capacitance. The dashed line shows a fit to **Equivalent circuit I**.

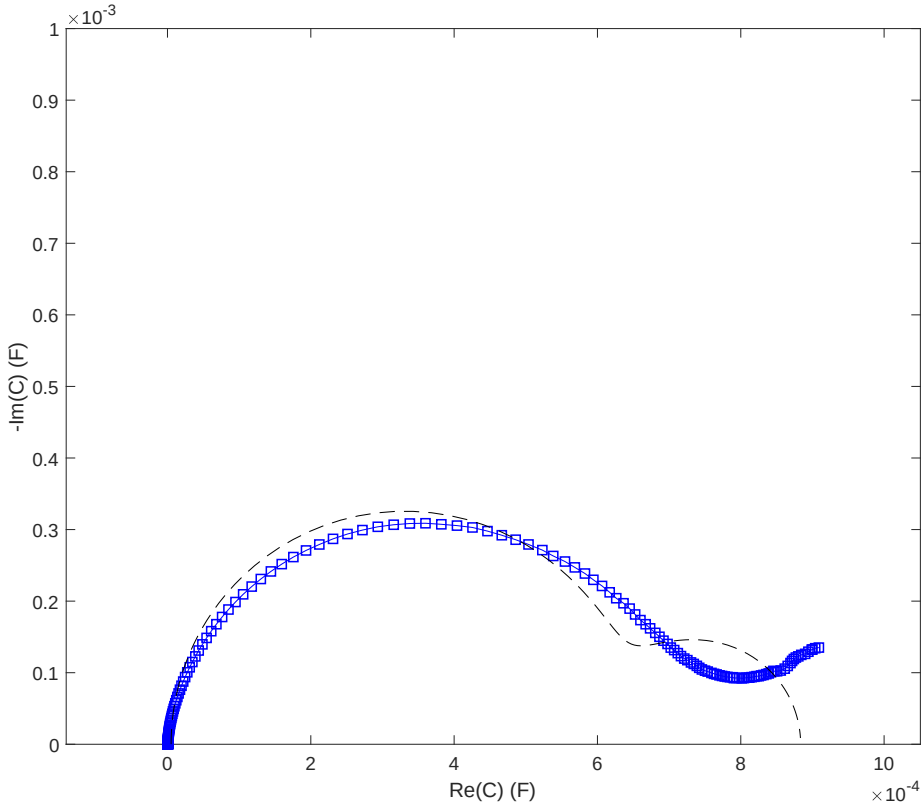

Figure S.12: Complex capacitance plot of a Ru@Pt/C catalyst at 0.5 V vs. RHE in 0.1 mol dm^{-3} $HClO_4$. The ohmic resistance was evaluated from the corresponding impedance-plane plot and subtracted from the data before calculating the complex capacitance. The dashed line shows a fit to **Equivalent circuit II**.

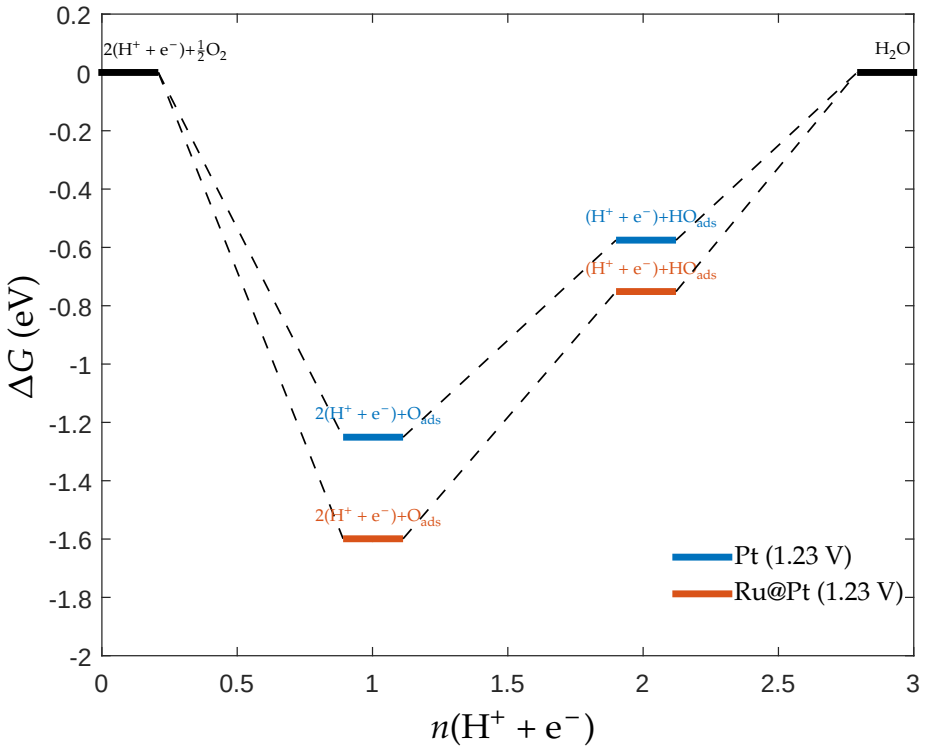

Figure S.13: Free energy diagram for the different reaction steps of the ORR at 1.23 V vs. RHE.